SCIENCE CHINA
Information Sciences

• RESEARCH PAPER •

February 2017, Vol. 60 022301:1–022301:9
doi: 10.1007/s11432-015-0979-5

CP-based MIMO OFDM radar IRCI free range reconstruction using real orthogonal designs

Tianxian ZHANG[1*], Xiang-Gen XIA[2] & Lingjiang KONG[1]

[1]*The School of Electronic Engineering, University of Electronic Science and Technology of China, Chengdu* 611731*, China;*
[2]*The Department of Electrical and Computer Engineering, University of Delaware, Newark, DE* 19716*, USA*

Received January 30, 2016; accepted May 23, 2016; published online November 8, 2016

Abstract In this paper, we propose a range reconstruction method for a frequency-band shared multiple-input multiple-output (MIMO) orthogonal frequency-division multiplexing (OFDM) radar with sufficient cyclic prefix (CP) by using real orthogonal designs. Compared with the application of complex orthogonal designs in our previous work, the application of real orthogonal designs can significantly reduce the number of the all-zero-valued pulses in a coherent processing interval (CPI) for each transmitter and increase the efficiency of radar transmitters. Meanwhile, it still maintains the advantages of full spatial diversity without inter-range-cell interference (IRCI). We also apply the rate-1 real orthogonal designs for different numbers of transmitters and pulses for range reconstruction without any idleness of radar transmitters. Simulation results are presented to illustrate the performances of the OFDM pulse design and the CP-based MIMO OFDM radar using real orthogonal designs.

Keywords cyclic prefix (CP), inter-range-cell interference (IRCI), multiple-input multiple-output (MIMO) radar, real orthogonal designs, orthogonal frequency division multiplexing (OFDM) pulse

Citation Zhang T X, Xia X-G, Kong L J. CP-based MIMO OFDM radar IRCI free range reconstruction using real orthogonal designs. Sci China Inf Sci, 2017, 60(2): 022301, doi: 10.1007/s11432-015-0979-5

1 Introduction

In recent years, multiple-input multiple-output (MIMO) radar has been widely investigated and applied in many radar applications [1–10]. According to different antenna configurations, MIMO radar can be generally divided into two types. The first type is colocated MIMO radar in which all the transmitted antennas and received antennas are located closely enough [1–4]. The second type is statistical MIMO radar that can obtain spatial diversity and improve the detection performance by using widely separated transmitters and receivers and observing a target from different spatial aspects [8–10]. To achieve spatial diversity, all the transmitted signals are usually assumed to be orthogonal to each other in time domain with arbitrary time delays and thus, they can be separated in each receiver. This assumption can hold if each transmitted antenna occupies a unique frequency band [11]. However, in this case, the frequency spectrum efficiency is low that reduces the radar range resolution. To overcome this issue, many works

* Corresponding author (email: tianxian.zhang@gmail.com)

have been focusing on a concept of frequency-band shared MIMO radar, in which they have relied on designing the time domain orthogonal codes/sequences [12–19]. However, all of these codes/sequences cannot accomplish ideal autocorrelations and cross-correlations with zero sidelobes. Thus, it would result in the spatial diversity and radar performance degradations.

In [20], we have proposed a frequency-band shared MIMO OFDM radar by using our designed OFDM pulses with sufficient length cyclic prefix (CP) [21, 22]. Different from most of the open literature about MIMO OFDM radar [23–25], the transmitted OFDM pulses of this CP-based MIMO OFDM radar are in the same frequency-band, while they are still orthogonal for each subcarriers in the discrete frequency domain with arbitrarily time delays. Therefore, the inter-range-cell interference (IRCI) free range reconstruction as well as the full spatial diversity can be achieved. In the proposed MIMO OFDM radar in [20], complex orthogonal designs [26, 27] are used to place the OFDM pulses across different transmitters to ensure the orthogonality of the waveforms across different transmitters in the discrete frequency domain. However, by using complex orthogonal designs, the number of the all-zero-valued pulses in a coherent processing interval (CPI) for each transmitter needs to be increased with the increase of the number of transmitters or transmitted pulses. Thus, this CP-based MIMO OFDM radar may suffer a low transmitter efficiency, especially, in case of long time coherent integration, which may cause problems in some radar applications (i.e., high transmitted peak power, long time transmitter idleness, and so on).

In this paper, we focus on the problem of frequency-band shared MIMO OFDM radar range reconstruction with sufficient length of CP by using real orthogonal designs. Firstly, we establish the signal model of CP-based MIMO OFDM radar with multiple OFDM pulses and analyze the problem of low transmitter efficiency as using complex orthogonal designs. Combining the real orthogonal designs, we also study the problem of radar range reconstruction and apply rate-1 real orthogonal designs for different numbers of transmitters and pulses. Finally, we present some simulations to demonstrate the performance benefits of the proposed CP-based MIMO OFDM radar by using real orthogonal designs. We find that, our proposed range reconstruction algorithm can avoid the idleness of radar transmitters, meanwhile, it maintains the advantage of full spatial diversity and IRCI free range reconstruction.

The rest of this paper is structured as follows. The CP-based MIMO OFDM radar signal model is established in Section 2. We then analyze the range reconstruction by using real orthogonal designs in Section 3. In Section 4, we show some simulation results. Finally, in Section 5, we conclude this paper.

2 Problem formulation

Consider a MIMO radar system with $\mathbb{T}$ fixed transmitters and $\mathbb{R}$ fixed receivers, which are located in a certain area. Consider that there are P coherent transmitted pulses within a radar CPI. In each pulse, there is an OFDM signal with a bandwidth of B Hz and N subcarriers. The time domain signal of the αth transmitted antenna as well as the pth OFDM pulse can be given by

$$s_{\alpha}^{(p)}(t) = \frac{1}{\sqrt{N}} \sum_{k=0}^{N-1} S_{\alpha,k}^{(p)} \exp\left\{ \mathrm{j}2\pi k \Delta f t \right\}, \ t \in [pT_r, pT_r + T + T_{GI}], \tag{1}$$

where T means the length of the OFDM signal within a single period but excluding CP. T_{GI} is the length of CP component. $\Delta f = \frac{B}{N} = \frac{1}{T}$ is the subcarrier spacing, T_r denotes the time interval between two successive pulses in one CPI. $\boldsymbol{S}_{\alpha}^{(p)} = [S_{\alpha,0}^{(p)}, S_{\alpha,1}^{(p)}, \ldots, S_{\alpha,N-1}^{(p)}]^{\mathrm{T}}, p = 0, 1, \ldots, P-1$ is the complex weights transmitted over the subcarriers of the α transmitter and pth OFDM pulse, and $(\cdot)^{\mathrm{T}}$ is the transpose. Without loss of generality, the total transmitted energy in one CPI is normalized to be 1, and assume that transmitted energy of each OFDM pulse is equal to $\sum_{k=0}^{N-1} |S_{\alpha,k}^{(p)}|^2 = \frac{1}{\mathbb{T}P}$ for all p and α.

After sampling at $t = pT_r + iT_{\mathrm{s}}$ within the time duration $t \in [pT_r, pT_r + T + T_{GI}]$ for $T = NT_{\mathrm{s}}$ and $T_{GI} = (\eta_{\max} + M - 1)T_{\mathrm{s}}$, the discrete complex envelope of the OFDM pulse in (1) can be written as

$$s_{\alpha,i}^{(p)} = s_{\alpha}^{(p)}(iT_{\mathrm{s}}) = \frac{1}{\sqrt{N}} \sum_{k=0}^{N-1} S_{\alpha,k}^{(p)} \exp\left\{ \frac{\mathrm{j}2\pi k i}{N} \right\}, \ i = 0, 1, \ldots, N + \eta_{\max} + M - 2, \tag{2}$$

where $T_{\rm s}$ is sampling interval length of the A/D converter, M is the number of range cells in the MIMO radar surveillance area. Within all of the transmitter and receiver pairs, the maximal relative time delay can be denote as $\eta_{\max}T_{\rm s}$ with

$$\eta_{\max} = \max_{\beta,\alpha}\{\eta_{\beta,\alpha}\}, \tag{3}$$

and the relative time delays between different transmitter and receiver pairs can be approximately denoted as $\eta_{\beta,\alpha}T_{\rm s}$ with $\eta_{\beta,\alpha} \in \mathbb{N}$, where $\mathbb{N}$ denotes the set of all natural numbers. Notice that the number subcarriers in a OFDM signal pulse should satisfy $N \geqslant \eta_{\max} + M$, at the same time, $s^{(p)}_{\alpha,i} = 0$ if $i < 0$ or $i > N + \eta_{\max} + M - 2$.

One way to avoid the interferences among different transmitted signals and achieve the full spatial diversity is to construct a $\mathbb{T} \times P$ row-orthogonal matrix $\boldsymbol{S}_k$:

$$\boldsymbol{S}_k = \begin{bmatrix} S^{(0)}_{1,k} & S^{(1)}_{1,k} & \cdots & S^{(P-1)}_{1,k} \\ S^{(0)}_{2,k} & S^{(1)}_{2,k} & \cdots & S^{(P-1)}_{2,k} \\ \vdots & \vdots & \ddots & \vdots \\ S^{(0)}_{\mathbb{T},k} & S^{(1)}_{\mathbb{T},k} & \cdots & S^{(P-1)}_{\mathbb{T},k} \end{bmatrix}, \tag{4}$$

satisfies $\boldsymbol{S}_k\boldsymbol{S}_k^{+} = \boldsymbol{I}_{\mathbb{T}}$ for every k, where $\boldsymbol{S}_k^{+} = \boldsymbol{S}_k^{\dagger}(\boldsymbol{S}_k\boldsymbol{S}_k^{\dagger})^{-1}$ is the Penrose-Moore pseudo-inverse of $\boldsymbol{S}_k$, $(\cdot)^{\dagger}$ denotes the conjugate transpose, and $\boldsymbol{I}_{\mathbb{T}}$ is the $\mathbb{T} \times \mathbb{T}$ identity matrix. By assuming $P \geqslant \mathbb{T}$, we have used the complex orthogonal designs to construct such $\boldsymbol{S}_k$ in [20]. For instance, when $(\mathbb{T}, P) = (4, 4)$, we use

$$\boldsymbol{S}_k = \begin{bmatrix} S^{(0)}_{1,k} & S^{(1)}_{1,k} & S^{(2)}_{1,k} & S^{(3)}_{1,k} \\ S^{(0)}_{2,k} & S^{(1)}_{2,k} & S^{(2)}_{2,k} & S^{(3)}_{2,k} \\ S^{(0)}_{3,k} & S^{(1)}_{3,k} & S^{(2)}_{3,k} & S^{(3)}_{3,k} \\ S^{(0)}_{4,k} & S^{(1)}_{4,k} & S^{(2)}_{4,k} & S^{(3)}_{4,k} \end{bmatrix} = \begin{bmatrix} S^{(0)}_{1,k} & S^{(1)}_{1,k} & S^{(2)}_{1,k} & 0 \\ -\left(S^{(1)}_{1,k}\right)^* & \left(S^{(0)}_{1,k}\right)^* & 0 & S^{(2)}_{1,k} \\ -\left(S^{(2)}_{1,k}\right)^* & 0 & \left(S^{(0)}_{1,k}\right)^* & -S^{(1)}_{1,k} \\ 0 & -\left(S^{(2)}_{1,k}\right)^* & \left(S^{(1)}_{1,k}\right)^* & S^{(0)}_{1,k} \end{bmatrix}, \quad k = 0, 1, \ldots, N-1, \tag{5}$$

where $(\cdot)^*$ denotes the complex conjugate. Notice that $\boldsymbol{S}_k$ can be used as the kth complex weights of P transmitted pulses within a single CPI of one transmitter, i.e., $[S^{(0)}_{1,k}, S^{(1)}_{1,k}, S^{(2)}_{1,k}, S^{(3)}_{1,k}]$ for the first transmitter as in (5). Meanwhile, $S^{(3)}_{1,k} = 0$ for $k = 0, 1, \ldots, N-1$. It indicates that there is one all-zero-valued transmitted pulse within a CPI of each transmitter as is shown in Figure 1. $\boldsymbol{s}^{(p)}_{\alpha} = [s^{(p)}_{\alpha,0}, \ldots, s^{(p)}_{\alpha,N-1}]^{\rm T}$ is the discrete time domain sequences for the pth OFDM pulse and the αth transmitter. $\boldsymbol{s}^{(p)}_{\alpha}$ can be obtained by taking the N-point IFFT of the sequence $\boldsymbol{S}^{(p)}_{\alpha} = [S^{(p)}_{\alpha,0}, \ldots, S^{(p)}_{\alpha,N-1}]^{\rm T}$. Notice that, when the complex conjugation in the frequency domain of a signal, it will cause the complex conjugation in the time domain of the signal, in the meantime, it will also cause the time reversal in the time domain. In Figure 1, $\prec \cdot \succ$ denotes a reversal of a sequence, i.e., $\prec \boldsymbol{s}^{(p)}_{\alpha} \succ = [s^{(p)}_{\alpha,0}, s^{(p)}_{\alpha,N-1}, \ldots, s^{(p)}_{\alpha,2}, s^{(p)}_{\alpha,1}]^{\rm T}$.

For a more general case with any $\mathbb{T}$ and P, $\boldsymbol{S}_k$ can be constructed by using complex orthogonal designs [26, 27]. However, according to the complex orthogonal designs in [26, 27], it is shown that there are at least

$$P_z = \frac{\lceil \frac{\mathbb{T}}{2} \rceil - 1}{2\lceil \frac{\mathbb{T}}{2} \rceil} P \tag{6}$$

zeros in each row of a complex orthogonal design, where $\lceil x \rceil$ denotes the smallest integer not less than x. Meanwhile, in the complex orthogonal designs, the locations of the P_z zeros in one row are different to any other rows. It means that there are P_z (almost $\frac{P}{2}$ for a large $\mathbb{T}$) all-zero-valued pulses in a CPI for each transmitter of the CP-based MIMO OFDM radar [20]. Thus, about half transmitting time of each transmitter is idle, which reduces the efficiency of radar transmitters. Moreover, to achieve the minimal P_z as in (6), the pulse number P should be significantly increased with the increase of $\mathbb{T}$ as in [26, Table I], for example, as $\mathbb{T} = 8$, 11, or 14, the minimal pulse number is $P = 56$, 792, or 6006, and the all-zero-valued pulses are at least $P_z = 35$, 462, or 3432, respectively. Thus, it will be a strong

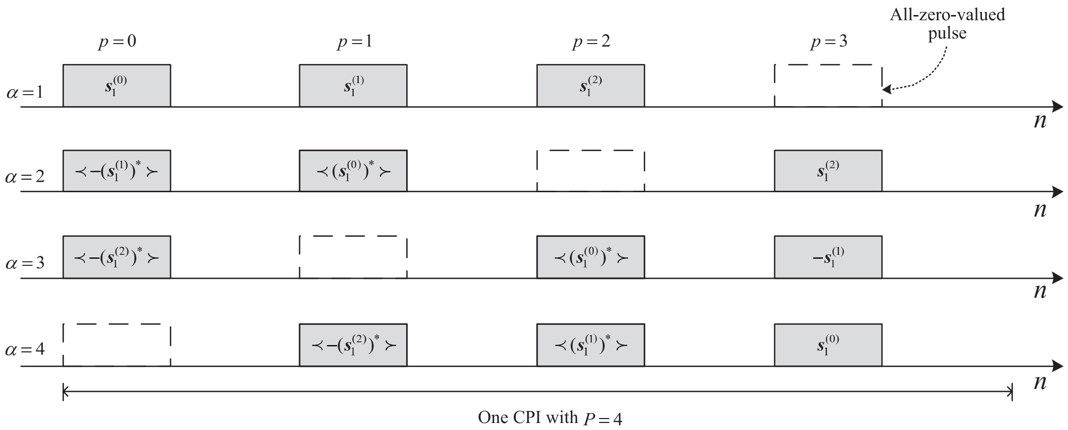

Figure 1 Illustration diagram of all transmitted pulses when using the complex orthogonal designs with $(\mathbb{T}, P) = (4, 4)$.

constraint for the choice of MIMO OFDM radar system parameters, especially, for radar with a large $\mathbb{T}$. These shortcomings using complex orthogonal designs might be a problem in some practical radar applications. Thus, it is important to obtain the range reconstruction without any idleness of radar transmitters for CP-based MIMO OFDM radar, and in the meantime it can still maintain the benefits of full spatial diversity and IRCI free range reconstruction. This is the main topic of the remainder of this paper.

3 Construct $\boldsymbol{S}_k$ using real orthogonal designs

To deal with the above issues, in this paper we use real orthogonal designs [28] to form $\boldsymbol{S}_k$, in which each row uses the same set of real variables. Consider a $\mathbb{T} \times P$ real orthogonal design with P real variables $x_0, x_1, \ldots, x_{P-1}$, which is a $\mathbb{T} \times P$ matrix $\boldsymbol{X}_{\mathbb{T},P}$ such that its every entry is either $-x_i$ or x_i, and in the meantime they satisfies the following identity:

$$\boldsymbol{X}_{\mathbb{T},P}\boldsymbol{X}_{\mathbb{T},P}^{\mathrm{T}} = (|x_0|^2 + |x_1|^2 + \cdots + |x_{P-1}|^2)\boldsymbol{I}_{\mathbb{T}}, \tag{7}$$

where every x_i may take any real value. A closed-form inductive design of a $\mathbb{T} \times P$ real orthogonal design for any $\mathbb{T}$ is proposed in [28]. For instance, when $(\mathbb{T}, P) = (2, 2)$ and $(\mathbb{T}, P) = (4, 4)$, the real orthogonal designs $\boldsymbol{X}_{2,2}$ and $\boldsymbol{X}_{4,4}$ can be, respectively, given by

$$\boldsymbol{X}_{2,2} = \begin{bmatrix} x_0 & x_1 \\ -x_1 & x_0 \end{bmatrix} \quad \text{and} \quad \boldsymbol{X}_{4,4} = \begin{bmatrix} x_0 & x_1 & x_2 & x_3 \\ -x_1 & x_0 & -x_3 & x_2 \\ -x_2 & x_3 & x_0 & -x_1 \\ -x_3 & -x_2 & x_1 & x_0 \end{bmatrix}. \tag{8}$$

With a real orthogonal design, a row-orthogonal matrix $\boldsymbol{S}_k$ can be constructed according to $\boldsymbol{X}_{\mathbb{T},P}$, and it guarantees $\boldsymbol{S}_k\boldsymbol{S}_k^{+} = \boldsymbol{I}_{\mathbb{T}}$. In [28], it is also inductively proved that, for any number of transmitters $\mathbb{T}$, a full rate-1 real orthogonal design $\boldsymbol{X}_{\mathbb{T},P}$ exists if $f(P) \geqslant \mathbb{T}$ with $P = 2^a(2b+1)$ and $f(P)$ is

$$f(P) = f\left(2^a\left(2b+1\right)\right) = \begin{cases} 8c+1, \text{ if } a = 4c, \\ 8c+2, \text{ if } a = 4c+1, \\ 8c+4, \text{ if } a = 4c+2, \\ 8c+8, \text{ if } a = 4c+3, \end{cases} \tag{9}$$

where a and b are integers, and $c = 0$ or $c \in \mathbb{N}$. With a real orthogonal design, such as (8), we only need to design P ($P = 4$ in (8)) pulses for the first transmitter to place at the positions of x_i as shown in (8). The pulses for other transmitters are either the same as or negatively signed copies of those at the first

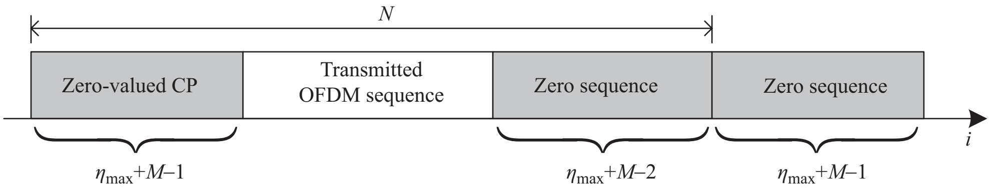

Figure 2 Illustration diagram of a time domain OFDM sequence of an OFDM pulse.

transmitter, which does not change their spectrum properties. Different from the complex orthogonal design case, there is not any zero in each row of a real orthogonal design. This means that there is not any all-zero-valued transmitted pulse in a CPI (i.e., $P_z = 0$), which guarantees the full efficiency for all radar transmitters. We also notice that there is no conjugate operation in the real orthogonal design. It means that no complex conjugation is needed in frequency domain sequence for the construction of $\boldsymbol{S}_k$ and no time domain reversal is necessary for the transmitted pulses of all radar transmitters. If there is no other requirement on the signal waveforms, for a set of P arbitrary real values $S_{1,k}^{(p)}$, $p = 0, 1, \ldots, P-1$, for any fixed k, with the above rate-1 real orthogonal design, the MIMO OFDM radar with sufficient CP proposed in [20] will provide an IRCI free range reconstruction with full spatial diversity. However, additional properties on the OFDM waveforms as used in [20] are needed for the MIMO radar as described below.

To achieve arbitrary length transmitted pulse and avoid transmitted energy redundancy, the CP part (length of $\eta_{\max} + M - 1$) of each time domain OFDM sequence can be designed to be zero as in [22]. Meanwhile, a real frequency domain sequence $\boldsymbol{S}_{\alpha}^{(p)}$ in the subcarrier direction as used in the above real orthogonal designs for all k requires a corresponding conjugate even time domain sequence $\boldsymbol{s}_{\alpha}^{(p)}$, e.g., $s_{\alpha,n}^{(p)} = \left(s_{\alpha,N-n}^{(p)}\right)^*$ for $n = 0, 1, \ldots, N-1$. Therefore, for each OFDM pulse, not only the head part (first $\eta_{\max} + M - 1$ elements) as in [20, 22] but also the tail part (last $\eta_{\max} + M - 2$ elements) of each time domain OFDM sequence within a single period N should be equal to zero as in Figure 2. Thus, the length of a transmitted OFDM pulse is $N_t T_{\mathrm{s}}$, where $N_t = N - 2\eta_{\max} - 2M + 3$, and the value of N_t can be arbitrary by choosing an arbitrary N. However, because of the conjugate even requirement for time domain sequence $\boldsymbol{s}_{\alpha}^{(p)}$ (or real value requirement for frequency domain sequence $\boldsymbol{S}_{\alpha}^{(p)}$), the number of free variable in $\boldsymbol{s}_{\alpha}^{(p)}$ (or $\boldsymbol{S}_{\alpha}^{(p)}$) for sequence design is reduced to half of that for sequence design by using complex orthogonal designs as in [20]. In this case, there will be less degrees of freedom for designing the OFDM pulse. We remark that, to achieve a complex orthogonal design with the maximum known rate $\frac{\lceil\frac{\mathbb{T}}{2}\rceil+1}{2\lceil\frac{\mathbb{T}}{2}\rceil}$, the value of P should be much larger than $\mathbb{T}$ when $\mathbb{T} > 4$ as in [26, Table I], for example, as $\mathbb{T} = 8$, the number of pulses should satisfy $P \geqslant 56$ to obtain a rate $\frac{5}{8}$ complex orthogonal design, while, according to the constraint in (9), for a given $\mathbb{T}$, a rate-1 real orthogonal design can be obtained with more flexible values of P, for example, as $\mathbb{T} = 8$, a rate-1 real orthogonal design can be obtained with $P = 8$, 16, 24, 32, 40, 48, or 56. Thus, by using real orthogonal designs, we have more choices of pulse number P for coherent integration in range reconstruction. Considering this feature, the real orthogonal designs might be more suitable for practical radar applications.

For joint OFDM pulse design, we adopt the modified iterative clipping and filtering (MICF) algorithm, which is reconfigured according to the corresponding algorithm in [20] as described in Algorithm 1 and Figure 3. Since real orthogonal designs are applied, all the frequency domain sequences of the designed OFDM pulses are required to be real, and this additional constraint is added to the MICF algorithm for the OFDM pulse design. Specifically, after the processing of "LN-point IFFT" as in Algorithm 1 and Figure 3, we obtain a time domain OFDM sequence $\tilde{\boldsymbol{s}}^{(p)}(q) \in \mathbb{C}^{LN} \times 1$ at the qth iteration, then, to obtain a real frequency domain OFDM sequence, we add a processing to sequence $\tilde{\boldsymbol{s}}^{(p)}(q)$ to achieve P conjugate even sequences, i.e.,

$$\bar{s}_n^{(p)}(q) = \frac{1}{2}\left[\tilde{s}_n^{(p)}(q) + \left(\tilde{s}_{LN-n}^{(p)}(q)\right)^*\right], \quad p = 0, 1, \ldots, P-1, \tag{10}$$

where $\tilde{s}_n^{(p)}(q)$ is the nth element of sequence $\tilde{\boldsymbol{s}}^{(p)}(q)$.

Algorithm 1: Summary of MICF

- Q is the pre-set maximum iteration number

Let $q = 0$;
Initialize the frequency domain sequences, i.e., $\boldsymbol{S}_\alpha^{(0)}(q), \boldsymbol{S}_\alpha^{(1)}(q), \dots, \boldsymbol{S}_\alpha^{(P-1)}(q)$;
while $q < Q$ **do**
  Pad $(L-1)N$ zeros to each frequency domain sequence;
  LN**-point IFFT** to each frequency domain sequence and obtain time domain sequences, i.e., $\tilde{\boldsymbol{s}}_\alpha^{(0)}(q), \tilde{\boldsymbol{s}}_\alpha^{(1)}(q), \dots, \tilde{\boldsymbol{s}}_\alpha^{(P-1)}(q)$;
  Construct the conjugate even time domain sequences, i.e., $\bar{\boldsymbol{s}}_\alpha^{(0)}(q), \bar{\boldsymbol{s}}_\alpha^{(1)}(q), \dots, \bar{\boldsymbol{s}}_\alpha^{(P-1)}(q)$;
  Time domain filtering by using "Filtering $\boldsymbol{h}$";
  Time domain clipping;
  LN**-point FFT** to each time domain sequence;
  Frequency domain filtering by using "Filtering $\boldsymbol{H}$";
  Frequency domain clipping;
  Let $q = q + 1$;
end while
N**-point IFFT** to each frequency domain sequence;
Time domain filtering by using "Filtering $\tilde{\boldsymbol{h}}$";
Energy normalization;
N**-point FFT** to each time domain sequence;
Output the frequency domain sequences $\boldsymbol{S}_\alpha^{(0)}, \boldsymbol{S}_\alpha^{(1)}, \dots, \boldsymbol{S}_\alpha^{(P-1)}$.

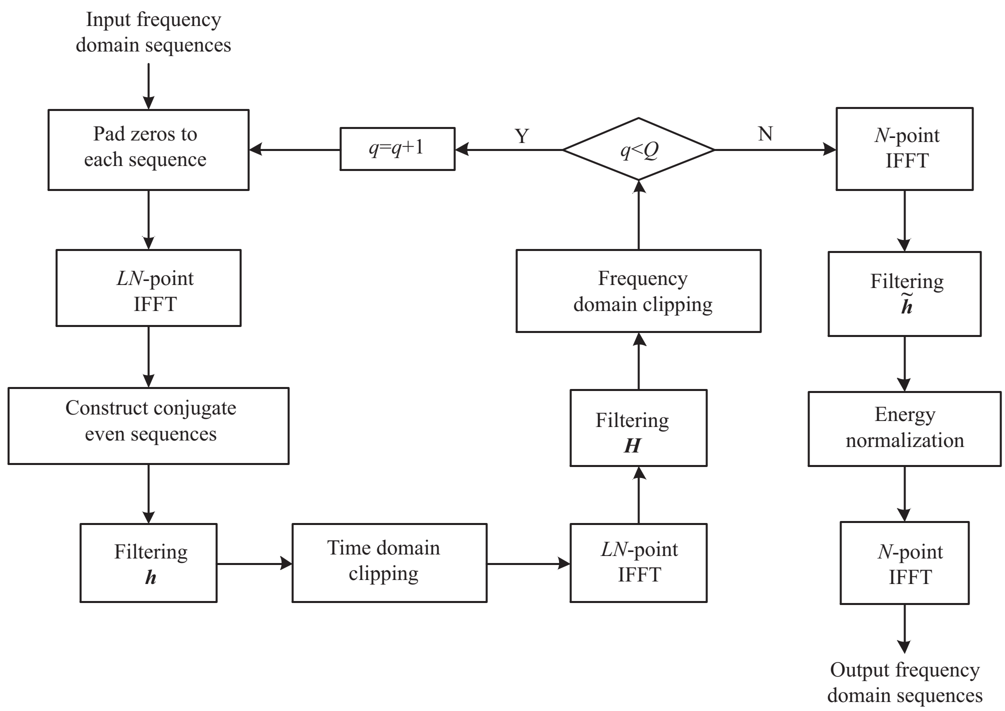

Figure 3 Block diagram of joint multiple real OFDM sequence design by applying MICF.

And then, the sequence $\bar{\boldsymbol{s}}^{(p)}(q) = [\bar{s}_0^{(p)}(q), \bar{s}_1^{(p)}(q), \dots, \bar{s}_{LN-1}^{(p)}(q)]^{\mathrm{T}}$ is used as the input of the processing "filtering $\boldsymbol{h}$" as in Algorithm 1 and Figure 3. In this case, after Q iterations, the P OFDM pulses can be obtained with real frequency domain sequences and suitable peak-to-average power ratio (PAPR) and signal-to-noise ratio (SNR) degradation factor ξ. To fairly compare the PAPR for using real and complex orthogonal designs, the PAPR here is defined over the whole P pulses including those all-zero-valued pulses, which is different with the PAPR defined only over the non-zero pulses as in [20]. Since in the two cases, the peak power has no difference, the only difference is the mean power that is calculated over the whole P pulses here while it is calculated only over the non-zero pulses in [20]. The detailed definitions about the "SNR degradation factor ξ", pre-set maximum iteration number "Q", and the following factors "G_f" and "PAPR_d" can be seen in [20].

We need to remark that, after acquiring the real frequency domain sequences $\boldsymbol{S}_\alpha^{(p)} = [S_{\alpha,0}^{(p)}, S_{\alpha,1}^{(p)}, \dots, S_{\alpha,N-1}^{(p)}]^{\mathrm{T}}$, for $\alpha = 1, 2, \dots, \mathbb{T}$ and $p = 0, 1, \dots, P-1$, the row-orthogonal matrix $\boldsymbol{S}_k$ can be formed as in (4). Then, the range reconstruction process for the CP-based MIMO OFDM radar (such as OFDM demodulation and coefficient estimation) is similar to that as in [20]. Due to the space limitation, we refer the reader to [20] for the details. We also remark that, in this paper, what we are most concerned about is the problem of transmitter idleness and narrow choices for system parameters in MIMO OFDM radar. By applying the real orthogonal designs in the range reconstruction for the CP-based MIMO OFDM radar, we can achieve IRCI free range reconstruction with more reasonable choices for radar system parameters (i.e., antenna number and pulse number). In the following section, we will focus on the performance evaluation for the algorithm of joint OFDM pulse design.

4 Simulation results

In this section, we will focus on the performance evaluation of the joint OFDM pulse design by adopting the MICF algorithm as in Algorithm 1 and Figure 3. The number of range cells is set as $M = 96$, the transmitted OFDM pulse length is $N_t = 33$ and the maximum relative time delays among different transmitters is set as $\eta_{\max} = 40$. Thus, the number of subcarriers is $N = N_t + 2\eta_{\max} + 2M - 3 = 302$. The over-sampling ratio is set as $L = 4$ to obtain a sufficiently accurate PAPR estimate as in [29, 30]. The pulse design performance is evaluated by investigating the PAPR of the P transmitted pulses as well as the SNR degradation factor ξ with 2000 independent standard Monte Carlo trials. In each trial, the initial frequency sequences (i.e., $\boldsymbol{S}_\alpha^{(p)}(0), \alpha = 1, 2, \dots, \mathbb{T}, p = 0, 1, \dots, P-1$) are set to be sequences constructed by the binary pseudo-random noise (PN) sequence with values of -1 and 1.

In Figures 4 and 5, we consider three cases with different numbers of pulses and transmitters (i.e., $\mathbb{T} = 2$, $P = 2$; $\mathbb{T} = 4$, $P = 4$; and $\mathbb{T} = 8$, $P = 56$) for joint OFDM pulse design. In all of these three cases, there is no all-zero-valued transmitted pulse in a CPI when applying real orthogonal designs (ROD) to construct $\boldsymbol{S}_k$. However, when applying complex orthogonal designs (COD) to construct $\boldsymbol{S}_k$, there are P_z all-zero-valued transmitted pulses within a CPI. Thus, the numbers of OFDM pulses for jointly free design are only $P - P_z$ as in [26], i.e., 2, 3 and 35 for these three cases, respectively. We also plot the cumulative distribution functions (CDF) for the SNR degradation factor ξ and the PAPR with $Q = 10$, $\text{PAPR}_d = 0.1$ dB and $G_f = 10\%$. The curves in Figure 4 indicate that the ξ is significantly improved with the increase of P. In Figure 5, the PAPR of OFDM pulse design when applying real orthogonal designs is worse than that using complex orthogonal designs for the cases of ($\mathbb{T} = 2$, $P = 2$). It is because that the number of free variables for OFDM pulse design as using real orthogonal designs is reduced to half of that for OFDM pulse design as using complex orthogonal designs. However, with the increase of P, the PAPR is degraded sharply as applying complex orthogonal designs, while, the PAPR is significantly improved as applying real orthogonal designs. It is because that, as using complex orthogonal designs, the number of all-zero-valued transmitted pulses is increased with the increase of $\mathbb{T}$ or P. It reduces the degrees of freedom for the OFDM pulse design, and in the meantime increases the PAPR of transmitted pulses. Nevertheless, there is no all-zero-valued transmitted pulse when applying real orthogonal designs.

Moreover, in Figure 5, the PAPR performance of OFDM pulse design by applying real orthogonal designs is improved when the numbers of $\mathbb{T}$ and P are increased. It is because, as using real orthogonal designs, there is no all-zero-valued pulses in transmission. When P is increased, the degrees of freedom in the OFDM pulse design would also be increased. However, the PAPR performance of OFDM pulse design by applying complex orthogonal designs is degraded when the numbers of $\mathbb{T}$ and P are increased. It indicates that, as using complex orthogonal designs, the number of all-zero-valued pulses is increased with the increase of $\mathbb{T}$ or P. It significantly reduces the degrees of freedom in the OFDM pulse design.

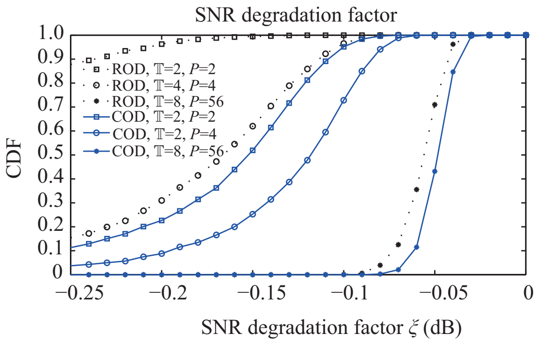

Figure 4 (Color online) CDFs of SNR degradation factor ξ for different $\mathbb{T}$ and P with $Q = 10$, $\mathrm{PAPR}_d = 0.1$ dB and $G_f = 10\%$.

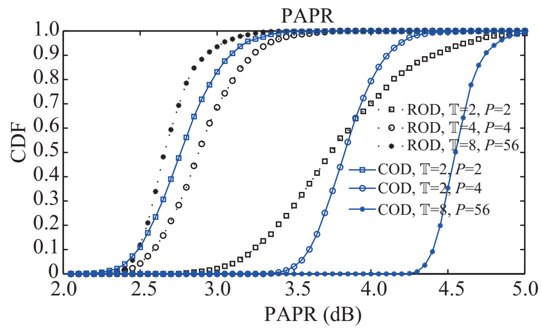

Figure 5 (Color online) CDFs of PAPR for different $\mathbb{T}$ and P with $Q = 10$, $\mathrm{PAPR}_d = 0.1$ dB and $G_f = 10\%$.

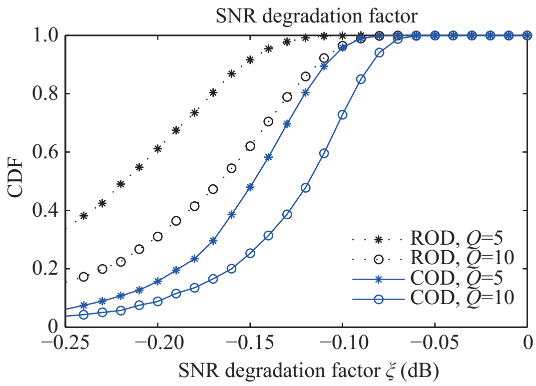

Figure 6 (Color online) CDFs of SNR degradation factor ξ for different Q with $\mathbb{T} = 4$, $P = 4$, $\mathrm{PAPR}_d = 0.1$ dB and $G_f = 10\%$.

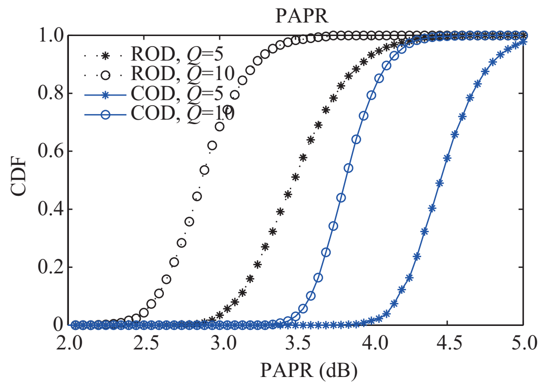

Figure 7 (Color online) CDFs of PAPR for different Q with $\mathbb{T} = 4$, $P = 4$, $\mathrm{PAPR}_d = 0.1$ dB and $G_f = 10\%$.

In Figures 6 and 7, we consider two cases with different maximum iteration numbers Q (i.e., $Q = 5$ and $Q = 10$) for joint OFDM pulse design. In both of these two cases, no matter when applying real orthogonal designs (ROD) or complex orthogonal designs (COD), the performances of the SNR degradation factor ξ and the PAPR are improved as Q is increased.

5 Conclusion

In this paper, we considered the problem of range reconstruction for a frequency-band shared CP-based MIMO OFDM radar by applying real orthogonal designs. With the real orthogonal designs, the CP-based MIMO OFDM radar not only can avoid the idleness of radar transmitters, but also can provide the benefit of IRCI free range reconstruction and full spatial diversity. We first gave the transmitted signal model and presented the idleness problem of radar transmitters as using complex orthogonal designs. We then considered the range reconstruction without any idleness of radar transmitters by using real orthogonal designs and applied rate-1 real orthogonal designs for different numbers of transmitters and pulses. By comparing with MIMO OFDM radar using complex orthogonal designs, we finally provided some simulations about OFDM pulse design to illustrate the benefits of the proposed algorithm, such as the significantly improved PAPR.

Acknowledgements This work was supported by National Natural Science Foundation of China (Grant Nos. 61501083, 61178068), Fundamental Research Funds of Central Universities (Grants No. ZYGX2015KYQD056), and Program for New Century Excellent Talents in University (Grant No. A1098524023901001063).

Conflict of interest The authors declare that they have no conflict of interest.

References

1 Li J, Stoica P. MIMO radar with colocated antennas. IEEE Signal Process Mag, 2007, 24: 106–114
2 Li J, Stoica P. MIMO Radar Signal Processing. New York: Wiley Online Library, 2008
3 Wu X H, Kishk A A, Glisson A W. MIMO-OFDM radar for direction estimation. IET Radar Sonar Nav, 2010, 4: 28–36
4 Cao Y-H, Xia X-G, Wang S-H. IRCI free co-located MIMO radar based on sufficient cyclic prefix OFDM waveforms. IEEE Trans Aerosp Electron Syst, 2015, 51: 2107–2120
5 Cao Y-H, Xia X-G. IRCI-free MIMO-OFDM SAR using circularly shifted Zadoff-Chu sequences. IEEE Geosci Remote Sens Lett, 2015, 12: 1126–1130
6 Meng C Z, Xu J, Xia X-G, et al. MIMO-SAR waveforms separation based on virtual polarization filter. Sci China Inf Sci, 2015, 58: 042301
7 He F, Chen Q, Dong Z, et al. Modeling and high-precision processing of the azimuth shift variation for spaceborne HRWS SAR. Sci China Inf Sci, 2013, 56: 102304
8 Haimovich A M, Blum R S, Cimini L J. MIMO radar with widely separated antennas. IEEE Signal Process Mag, 2008, 25: 116–129
9 Chernyak V. Multisite radar systems composed of MIMO radars. IEEE Aerospace Electron Syst Mag, 2014, 29: 28–37
10 Xu J, Dai X-Z, Xia X-G, et al. Optimizations of multisite radar system with MIMO radars for target detection. IEEE Trans Aerospace Electron Syst, 2011, 47: 2329–2343
11 Antonio G S, Fuhrmann D R, Robey F C. MIMO radar ambiguity functions. IEEE J Sel Topics Signal Process, 2007, 1: 167–177
12 Somaini U. Binary sequences with good autocorrelation and cross correlation properties. IEEE Trans Aerospace Electron Syst, 1975, 11: 1226–1231
13 Deng H. Synthesis of binary sequences with good autocorrelation and crosscorrelation properties by simulated annealing. IEEE Trans Aerospace Electron Syst, 1996, 32: 98–107
14 Deng H. Polyphase code design for orthogonal netted radar systems. IEEE Trans Signal Process, 2004, 52: 3126–3135
15 Khan H A, Zhang Y Y, Ji C L, et al. Optimizing polyphase sequences for orthogonal netted radar. IEEE Signal Process Lett, 2006, 13: 589–592
16 He H, Stoica P, Li J. Designing unimodular sequence sets with good correlations-Including an application to MIMO radar. IEEE Trans Signal Process, 2009, 57: 4391–4405
17 Song X F, Zhou S L, Willett P. Reducing the waveform cross correlation of MIMO radar with space-time coding. IEEE Trans Signal Process, 2010, 58: 4213–4224
18 Xu L, Liang Q L. Zero correlation zone sequence pair sets for MIMO radar. IEEE Trans Aerospace Electron Syst, 2012, 48: 2100–2113
19 Jin Y, Wang H, Jiang W, et al. Complementary-based chaotic phase-coded waveforms design for MIMO radar. IET Radar Sonar Nav, 2013, 7: 371–382
20 Xia X-G, Zhang T X, Kong L J. MIMO OFDM radar IRCI free range reconstruction with sufficient cyclic prefix. IEEE Trans Aerospace Electron Syst, 2015, 51: 2276–2293
21 Zhang T X, Xia X-G. OFDM synthetic aperture radar imaging with sufficient cyclic prefix. IEEE Trans Geosci Remote Sens, 2015, 53: 394–404
22 Zhang T X, Xia X-G, Kong L J. IRCI free range reconstruction for SAR imaging with arbitrary length OFDM pulse. IEEE Trans Signal Process, 2014, 62: 4748–4759
23 Kim J-H, Younis M, Moreira A, et al. A novel OFDM chirp waveform scheme for use of multiple transmitters in SAR. IEEE Geosci Remote Sens Lett, 2013, 10: 568–572
24 Sit Y L, Sturm C, Baier J, et al. Direction of arrival estimation using the MUSIC algorithm for a MIMO OFDM radar. In: Proceedings of IEEE Radar Conference, Atlanta, 2012. 0226–0229
25 Sen S, Nehorai A. OFDM MIMO radar with mutual-information waveform design for low-grazing angle tracking. IEEE Trans Signal Process, 2010, 58: 3152–3162
26 Lu K J, Fu S L, Xia X-G. Closed-form designs of complex orthogonal space-time block codes of rates $(k+1)/(2k)$ for $2k-1$ or $2k$ transmit antennas. IEEE Trans Inf Theory, 2005, 51: 4340–4347
27 Liang X-B. Orthogonal designs with maximal rates. IEEE Trans Inf Theory, 2003, 49: 2468–2503
28 Geramita A V, Seberry J. Orthogonal Designs, Quadratic Forms and Hadamard Matrices, Lecture Notes in Pure and Applied Mathematics, Vol. 43. New York and Basel: Marcel Dekker, 1979
29 Armstrong J. Peak-to-average power reduction for OFDM by repeated clipping and frequency domain filtering. Electron Lett, 2002, 38: 246–247
30 Han S H, Lee J H. An overview of peak-to-average power ratio reduction techniques for multicarrier transmission. IEEE Wirel Commun, 2005, 12: 56–65